

# A PHASE MATCHING, ADIABATIC ACCELERATOR \*

F. Lemery<sup>1,2†</sup>, K. Floettmann<sup>3</sup>, P. Piot<sup>4,5‡</sup>, F. X. Kaertner<sup>1,2,6</sup>

<sup>1</sup> Department of Physics, University of Hamburg, Jungiusstrasse 9, 20355 Hamburg, Germany

<sup>2</sup> Center for Free-Electron Laser Science (CFEL), DESY, Notkestrasse 85, 22607 Hamburg, Germany

<sup>3</sup> DESY, Notkestrasse 85, 22607 Hamburg, Germany

<sup>4</sup> Department of Physics, and Northern Illinois Center for Accelerator & Detector Development, Northern Illinois University DeKalb, IL 60115, USA

<sup>5</sup> Fermi National Accelerator Laboratory, Batavia, IL 60510, USA

<sup>6</sup> The Hamburg Center for Ultrafast Imaging, Luruper Chaussee 149, 22761 Hamburg, Germany

## Abstract

Tabletop accelerators are highly sought after. One way of reducing accelerator footprints is to down-scale electromagnetic wavelengths; however, without correspondingly high field gradients, particles will be more susceptible to phase-slippage – especially at low energy. We investigate how an adiabatically-tapered dielectric-lined waveguide could maintain phase-matching between the accelerating mode and electron bunch at moderate field strength. We describe our analytical model, compare it with CST and implement it into ASTRA and provide a glimpse into the beam dynamics.

## INTRODUCTION

Particle accelerators have emerged as essential tools to explore fundamental science. Particle colliders for example, have extended our knowledge of the fundamental forces and essentially contributed to the development of the standard model. More recently, the advent of light sources based on synchrotron radiation from high-energy (GeV) electron bunches has extended our vision to Angstrom-scale interactions, allowing us to peer onto biological and chemical interactions at femtosecond timescales. Electron-diffraction imaging offers a significantly lower-energy route ( $\sim$ MeV) to observing Angstrom-scale phenomena with unprecedented resolution.

Exploring smaller and faster processes generally requires more energetic particle beams which has driven the development of large-scale accelerators such as the LHC, LCLS, and European XFEL. Modern accelerators are based on radio frequency (RF) technology with wavelengths on  $O(10$  cm) and corresponding accelerating gradients  $O(100$  MV/m). Scaling to smaller wavelengths has its own complications. A shorter wavelength requires a relatively short bunch ( $\sigma_z \ll \lambda$ ) to maintain reasonable energy spreads under acceleration. Moreover, from the normalized vector potential  $a_0 \propto E_0 \lambda$ , obtaining the same acceleration dynamics in a scaled accelerator requires  $E_0 \propto \lambda^{-1}$  [1]. Realizing GV/m+ acceleration gradients is difficult and also presents challenges such as tight tolerances and breakdowns [2] in metallic structures.

\* This work was supported by the European Research Council (ERC) under the European Union's Seventh Framework Programme (FP/2007-2013)/ERC Grant agreement no. 609920

† francois.lemery@gmail.com

‡ PP was funded by NSF grant PHY-1535401 with NIU

These limitations have motivated research into alternative acceleration techniques which fall into two general categories operating in sub-millimeter-scale regimes: beam-driven and laser-driven acceleration. Beam-driven acceleration uses a high-impedance medium (e.g. dielectric lined waveguide (DLW) or plasma) to transfer energy between two ultrarelativistic bunches [3]. In laser-driven acceleration, a high-power laser is used to accelerate an electron bunch either directly (i.e. direct laser acceleration (DLA) [4, 5]) or via a medium e.g. plasmas [6, 7]. A principle limitation to these techniques is phase-slippage where the accelerating electron bunch velocity is not matched to the phase velocity ( $v_p$ ) of the structure or plasma. In the ultrarelativistic limit this problem is mitigated; however, acceleration at low energies has been predominately accomplished with an ultra-high power laser pulse in the multi-TW regime.

Here we describe a technique to abridge low-energy acceleration with small wavelengths *and* relatively small accelerating fields. We accomplish this with an adiabatically-tapered DLW to maintain phase matching between the longitudinally-dependent phase velocity of the structure and the accelerating electron bunch. We discuss the general theory of the structure, its limitations, we provide an example with  $\lambda = 1$  mm and discuss the resulting beam dynamics.

## THEORY

Dielectric-lined waveguides (DLWs) have attracted interest in the accelerator community for their versatility to accelerate, manipulate and characterize [8–13] electron beams. A DLW is generally composed of a hollow core surrounded by a dielectric lining with an outer metallic coating. Here we consider a cylindrical-DLW with inner radius  $a$ , outer radius  $b$  and relative dielectric permittivity  $\epsilon_r$ . The accelerating (TM<sub>01</sub>) mode has the following general field solutions in cylindrical coordinates  $(r, \phi, z)$  [14]

$$\begin{aligned} E_z &= E_0 I_0(rk_1) \sin(\omega t - k_z z + \psi) \\ E_r &= \frac{E_0 k_z}{k_1} I_1(rk_1) \cos(\omega t - k_z z + \psi) \\ H_\phi &= \frac{\omega \epsilon_0 E_0}{k_1} I_1(rk_1) \cos(\omega t - k_z z + \psi), \end{aligned} \quad (1)$$

where  $k_1 = \omega \sqrt{\frac{1}{v_p^2} - \frac{1}{c^2}}$ ,  $k_2 = \omega \sqrt{\frac{\epsilon_r}{c^2} - \frac{1}{v_p^2}}$ , and  $k_z = \frac{\omega}{v_p}$ . Here  $I$  is the modified Bessel function of the first kind,  $E_0$  is the longitudinal field amplitude,  $k_1$  and  $k_2$  are the radial components of the wavenumber  $k$  in the vacuum core and dielectric respectively,  $k_z$  is the longitudinal wavenumber,  $v_p$  is the phase velocity,  $\omega$  is the angular frequency and  $\psi$  is a phase constant. Solutions to the characteristic equation depend on the DLW structure parameters ( $a, b, \epsilon_r$ ) and yield propagating modes for  $(\omega, k_z)$ .

We make the following ansatz for the fields in a tapered waveguide

$$\begin{aligned} E_z &= E_0 I_0(rk_1) \sin(\omega t - \int_0^z dz k_z + \psi) \\ E_r &= \frac{E_0 k_z}{k_1} I_1(rk_1) \cos(\omega t - \int_0^z dz k_z + \psi) \\ H_\phi &= \frac{E_0 \omega \epsilon_0}{k_1} I_1(rk_1) \cos(\omega t - \int_0^z dz k_z + \psi), \end{aligned} \quad (2)$$

where  $E_0$ ,  $k_1$  and  $k_z$  now depend on  $z$ . Checking with Maxwell's equations,

$$\begin{aligned} \frac{\partial}{\partial z} E_z &= -\frac{1}{r} \frac{\partial}{\partial r} (r E_r), \\ \frac{\partial}{\partial t} \frac{E_z}{c^2} &= -\frac{1}{r} \frac{\partial}{\partial r} (r B_\phi), \end{aligned} \quad (3)$$

the ansatz is satisfied and adiabatic for the following conditions

$$\begin{aligned} \left| \frac{r k_1' I_1(k_1 r)}{k_z I_0(k_1 r)} \right| &= \left| \frac{v_p'}{\sqrt{1 - v_p^2}} r \frac{I_1(k_1 r)}{I_0(k_1 r)} \right| \ll 1, \\ \left| \frac{E_0'}{E_0 k_z} \right| &= \left| \frac{E_0' v_p}{E_0 \omega} \right| \ll 1. \end{aligned} \quad (4)$$

To include particle acceleration, we solve the coupled differential equations

$$\begin{aligned} \frac{\partial z}{\partial t} &= \beta c \\ \frac{\partial \beta}{\partial t} &= \frac{e E_0}{\gamma^3 m c} \sin(\omega t - \int_0^z k_z dz + \phi). \end{aligned} \quad (5)$$

We developed a C++ code to iteratively solve the dispersion relations and field equations; for a given inner radius  $a$ , we solve the system of equations to obtain  $E_0$  and the appropriate taper thickness  $\delta$  at a particular  $v_p$ ; now however,  $v_p$  corresponds to the normalized velocity of the accelerating particle  $\beta$ . We implemented our ansatz field equations into ASTRA [15]. In the following section we discuss simulation results for a 300 GHz, 100 MV/m structure.

## $\lambda=1$ mm, $E_0=100$ MV/m EXAMPLE

We now consider an example based on a 300 GHz ( $\lambda=1$  mm) driving field in a structure with constant inner radius  $a = 0.5$  mm and varying  $b$  made of Quartz ( $\epsilon_r = 4.41$ ) – limiting  $v_p > c/\sqrt{\epsilon_r} \sim .48c$ . We consider a bunch with initial energy of  $\mathcal{E}_i=205$  keV, corresponding to  $\beta = 0.7$ .

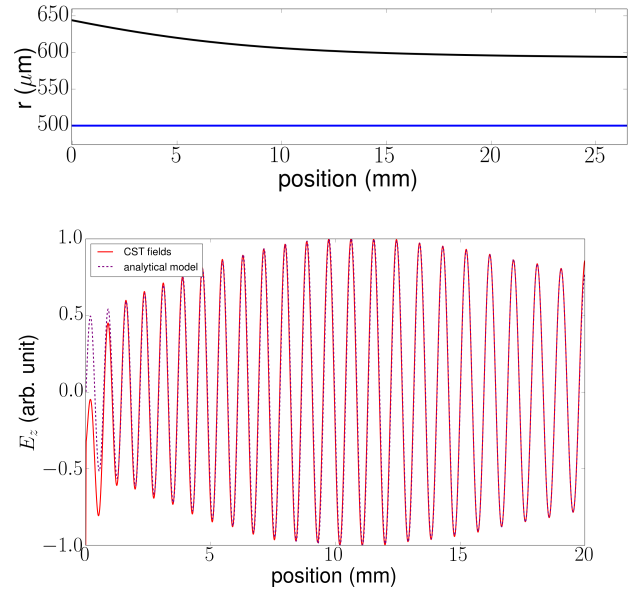


Figure 1: The tapered structure in our example for a fixed inner radius  $a=0.5$  mm (blue) and a tapered Quartz ( $\epsilon_r = 4.41$ ) dielectric thickness with outer radius (shown red). The taper is matched for an initial energy of  $\mathcal{E}_i=205$  keV with a maximum accelerating field of  $E_0=100$  MV/m. We show the comparison with CST-MWS (bottom) for completeness.

The structure (shown in Fig. 1(top)) is matched to  $E_0=100$  MV/m (note  $E_0=100$  MV/m for  $v_p = c$  (e.g.  $k_1 = 0$ ), at  $z = 0$  where  $v_p = 0.7c$ ,  $E_0 \sim 20$  MV/m). From Eq. 4 the condition for  $r=100 \mu\text{m}$  at  $z=0$  gives 0.0017 and approaches  $10^{-7}$  toward the end of the structure. For completeness we compared our analytical model with CST MWS [16] (see Fig. 1(bottom)) for the first 2 cm of the structure where the majority of the taper occurs; discrepancies arise at the entrance and exit of the structure which are excluded in our theoretical model.

We can gain some insights into the longitudinal dynamics with a single particle; illustrated in Fig. 2(top), the final energy is plotted as a function of the injection phase for various accelerating fields; larger gradients enable a larger acceptance while no efficient acceleration is possible for lower gradients. Fig. 2(bottom) shows the end phase as a function of starting phase, a plateau in the curve implies the end phase is within a certain interval independent of the initial phase, i.e. the bunch is compressed.

Finally we look at the acceleration dynamics of a 100 fC spherical electron bunch radius  $\sigma_r=10 \mu\text{m}$  with zero emittance and energy spread. We used a 1.2 T magnetic field to counter the defocussing forces. We scan over the in-

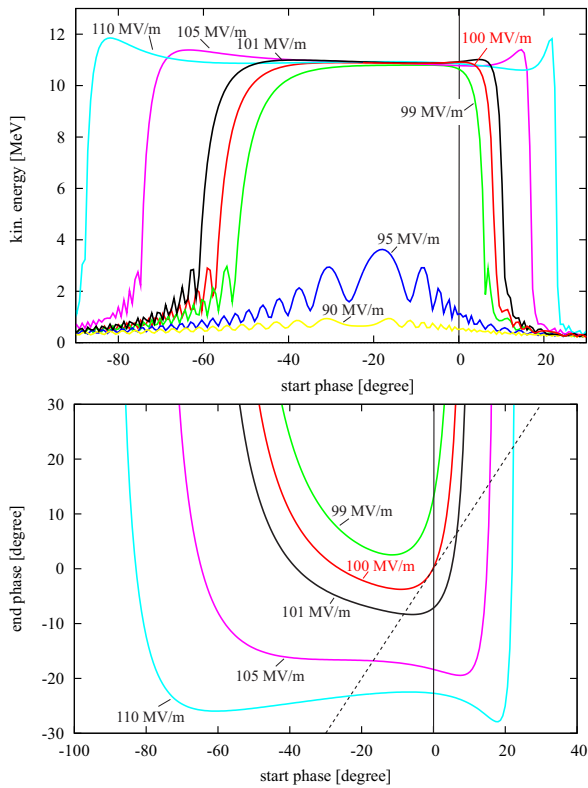


Figure 2: A phase scan (top) illustrating the final energy as a function of initial phase for various accelerating fields for a structure matched to 100 MV/m. The larger accelerating gradients have a larger dynamical range of acceleration trajectories; leading to larger acceptances for initial phases. Bottom figure shows the end phase as a function of initial phase for various accelerating gradients for a structure matched to 100 MV/m. Plateaus e.g. semi-constant end phases suggests the bunch is compressed. No compression or decompression requires a linear curve with derivative 1. Along the dashed line the end phase is equal to the start phase, i.e., the phase stays constant for only a small interval around 0° in the 100 MV/m curve.

jection phase  $\phi$  and maximum accelerating field  $E_0$  (see Fig. 3); while the maximum energy of the structure is fixed by  $v_p(z)$  of the structure, other beam parameters e.g.  $\sigma_z$ ,  $\epsilon_{\perp}$ ,  $\sigma_E$  are quite versatile over  $(E_0, \phi)$ . For example we find that for  $(E_0, \phi)=(110\text{MV/m}, 18^\circ)$  yields final parameters  $\sigma_z=1.2 \mu\text{m}$ ,  $\epsilon_{\perp}=0.15 \pi \text{ mm mrad}$ ,  $\sigma_E=60 \text{ keV}$ , or with  $(E_0, \phi)=(108\text{MV/m}, 24^\circ)$  yields final parameters  $\sigma_z=3 \mu\text{m}$ ,  $\epsilon_{\perp}=0.07 \pi \text{ mm mrad}$ ,  $\sigma_E=0.11 \text{ keV}$ .

### CONCLUSION

We have described a new method of accelerating low-energy particles by maintaining phase-matching between an accelerating bunch and the phase of the longitudinal electric field with an adiabatically tapered dielectric lined waveguide. We developed an analytical model which was validated with Maxwell's equations and CST MWS. The analytical model was implemented into ASTRA and we provide a beam dynam-

ics example. Our future work will look at other e.g. slab structures; and optimizations. We also investigate ways to reduce the required magnetic field strengths.

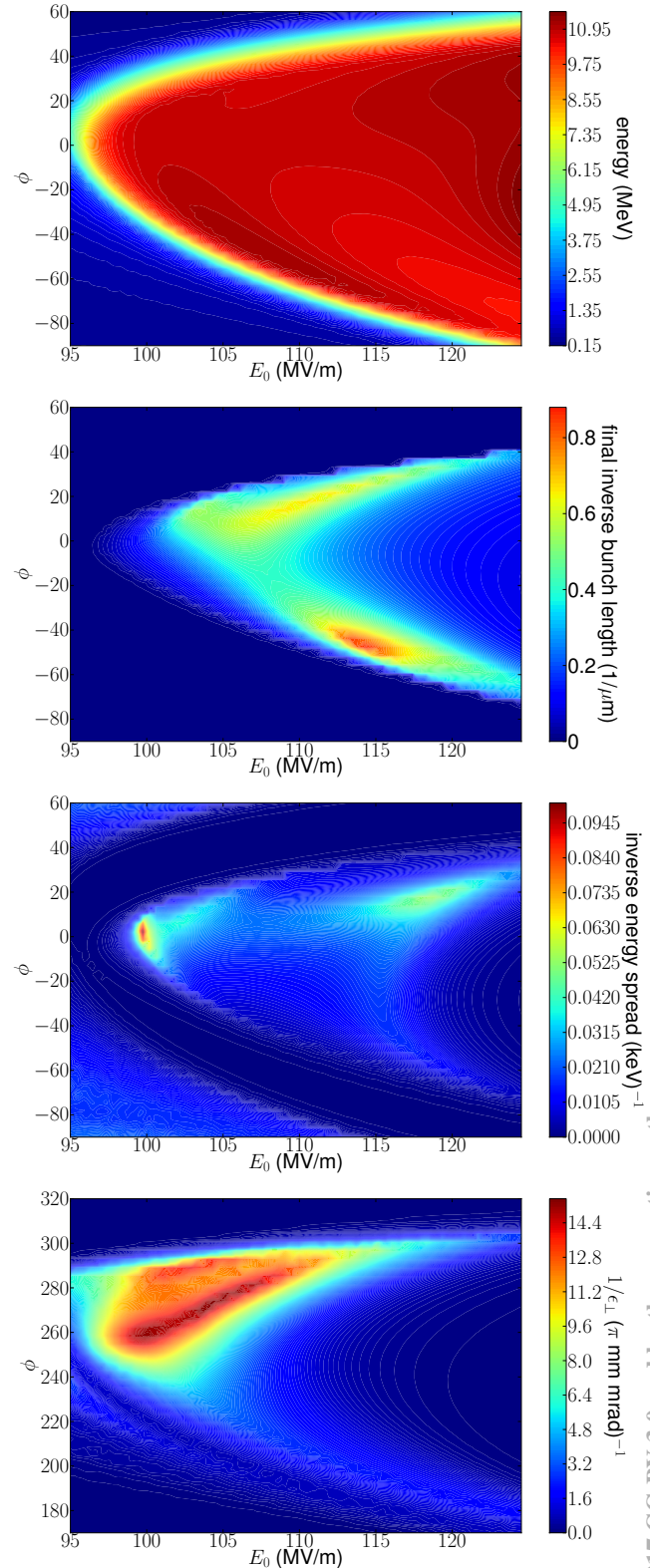


Figure 3: Scan results over  $(E_0, \phi)$  for a structure matched for 100 MV/m with  $\lambda=1 \text{ mm}$ .

## REFERENCES

- [1] J. Rosenzweig, E. Colby, "Charge and wavelength scaling of RF photoinjectors", in *Proc. PAC 1995*, Dallas, Texas, USA, May 1995, paper WPB05, pp. 957-960.
- [2] M. Dal Forno, V. Dolgashev *et al.*, "RF breakdown tests of mm-wave metallic accelerating structures", *Phys. Rev. Accel. Beams*, vol. 19, 011301 (2016).
- [3] G. A. Voss and T. Weiland, DESY Hamburg Report No. DESY-M-82-10, 1982.
- [4] T. Plettner, R. L. Byer, and B. Montazeri, "Electromagnetic forces in the vacuum region of laser-driven layered grating structure", *J. Mod. Opt.* 58, 1518 (2011).
- [5] J. Breuer and P. Hommelhoff, "Laser-Based Acceleration of Nonrelativistic Electrons at a Dielectric Structure", *Phys. Rev. Lett.* 111, 134803 (2013).
- [6] K. Nakajima, *et al.*, "Observation of Ultrahigh Gradient Electron Acceleration by a Self-Modulated Intense Short Laser Pulse", *Phys. Rev. Lett.* 74, 22 (1995).
- [7] C. G. R. Geddes, *et al.*, "High-quality electron beams from a laser wakefield accelerator using plasma-channel guiding", *Nature* 431, 538-441 (2004).
- [8] W. Gai *et al.*, "Experimental Demonstration of Wake-Field Effects in Dielectric Structures", *Phys. Rev. Lett.* 61, 2756 (1998).
- [9] Nanni, E. A. *et al.*, "Terahertz-driven linear electron acceleration", *Nat. Commun.* 6:8486 doi: 10.1038/ncomms9486 (2015).
- [10] P. Craievich, "Passive longitudinal phase space linearizer", *Phys. Rev. Accel. Beams* 13, 034401 (2010).
- [11] F. Lemery and P. Piot, "Ballistic bunching of photoinjected electron bunches with dielectric-lined waveguides", *Phys. Rev. Accel. Beams* 17, 112804 (2014).
- [12] G. Andonian *et al.*, "Bunch profile shaping using beam self-wakefields in a dielectric structure", *AIP Conference Proceedings* 1777, 070002 (2016).
- [13] F. Lemery and P. Piot, "Considerations for an Efficient Terahertz-Driven Electron Gun", in *Proc. IPAC'15*, Richmond, VA, USA, paper WEPWA070, pp. 2664-2666.
- [14] Roger F. Harrington, "Time-Harmonic Electromagnetic Fields", New York, NY: Wiley, 1961. Print.
- [15] ASTRA, K.Floettmann, <https://www.desy.de/~mpyflo/>
- [16] CST STUDIO SUITE, <https://www.cst.com>